Electron-Ion Plasma Modification of Al-based Alloys

Yurii Ivanov[1, 2, 3, a)], Mariya Rygina[3, b)], Elizaveta Petrikova[1, 2, c)], Olga Krysina[1, 2, d)], Anton Teresov[1, 2, e)], Olga Ivanova[4, f)] and Irina Ikonnikova[4, g)]

[1]*Institute of High-Current Electronics of the Siberian Branch of the Russian Academy of Sciences, 634055, Russia, Tomsk, 2/3 Akademicheskiy Ave.*
[2]*National Research Tomsk State University, 634050, Russia, Tomsk, 36 Lenina Str.*
[3]*National Research Tomsk Polytechnic University, Tomsk, 634050, Russia, Tomsk, 30 Lenina Str.*
[4]Tomsk State University of Architecture and Building, Tomsk, 634002, Russia, Tomsk, 2 Solyanaya Sq.

[a)] Corresponding author: yufi55@mail.ru
[b)] l-7755me@mail.ru; [c)] elizmarkova@yahoo.com; [d)] krysina_82@mail.ru; [e)] tad514@sibmail.com;
[f)] ivaov@mail.ru; [g)] irina-ikonnikova@yandex.ru

Abstract. The paper reports on the study where we analyzed the surface structure and strength properties of coated Al alloys modified by electron-ion plasma treatment. The Al alloys were deposited with a thin (≈0.5 μm) TiCu film coating (TiCu-Al system) and with a hard TiCuN coating (TiCuN–AlSi system) on a TRIO vacuum setup in the plasma of low-pressure arc discharges. The temperature fields and phase transformations in the film–substrate system were estimated by numerical simulation in a wide range of electron energy densities (5–30 J/cm^2) and pulse durations (50–200 μs). The calculations allowed us to determine the threshold energy density and pulse duration at which the surface structure of the irradiated Al-based systems is transformed in a single-phase state (solid or liquid) and in a two-phase state (solid plus liquid). The elemental composition, defect structure, phase state, and lattice state in the modified surface layers were examined by optical, scanning, and transmission electron microscopy, and by X-ray diffraction analysis. The mechanical characteristics of the modified layers were studied by measuring the hardness and Young's modulus. The tribological properties of the modified layers were analyzed by measuring the wear resistance and friction coefficient. It is shown that melting and subsequent high-rate crystallization of the TiCu–Al system makes possible a multiphase Al-based surface structure with the following characteristics: crystallite size ranging within micrometer, microhardness of more than 3 times that in the specimen bulk, and wear resistance ≈1.8 times higher compared to the initial material. Electron beam irradiation of the TiCuN–AlSi system allows fusion of the coating into the substrate, thus increasing the wear resistance of the material ≈2.2 times at a surface hardness of ~14 GPa.

INTRODUCTION

Aluminum has a number of advantages, including high specific strength, resistance to corrosion and flame, seismic stability, strength stability at negative temperatures, and small specific weight [1]. Aluminum alloys remain the main engineering materials in aerospace industry, automobile industry, and shipbuilding [1, 2]. The main disadvantages of aluminum are in its low elastic modulus, low hardness, and low strength. For this reason aluminum is rarely used in its pure form and is more often alloyed with different materials. Reasoning from the deficit and high cost of alloying elements, which greatly increase the price of high alloys, it is economically and technologically beneficial to develop a radically new approach to creation of materials in which low alloys provide desired mechanical and tribological properties, while special surface features are provided by continuously or locally doped thin surface layers and coatings. The new approach is particularly urgent for modification of light Al alloys whose low tribological and strength properties are barrier to their wider application in different fields of industry, in particular in aerospace. The approach is used in a series of methods (e.g. continuous laser powder cladding [3], pulsed plasma treatment [4], high-dose implantation [5], diffusion solid-phase mixing of multilayer thin films [6], diffusion saturation from gas discharge plasmas [7] and compression plasmas [8]) and allows surface treatment with

Advanced Materials in Technology and Construction (AMTC-2015)
AIP Conf. Proc. 1698, 030012-1–030012-7; doi: 10.1063/1.4937834

the formation of nanosized metastable phases, nanocomposites, and intermetallic compounds featuring unique physicochemical and service properties.

The paper describes the study where we analyzed the temperature fields, surface structure, and strength properties of commercially pure aluminum and aluminum-silicon alloy modified by electron-ion plasma treatment.

MATERIALS AND METHODS

In the study we used two Al alloys: commercially pure aluminum of grade A7 (Al) and Al-based alloy of grade AK12 with 12 % of Si (AlSi) [1]. Test specimens were treated in two stages [9]. At the first stage, the Al specimens were deposited with a thin Ti12%Cu film ≈0.5 μm thick (TiCu–Al system) and the AlSi specimens were deposited with hard TiCuN coating ≈0.5 μm thick (TiCuN–AlSi system); the deposition was realized on a TRIO setup by vacuum arc sputtering in the plasma of low-pressure arc discharge. At the second stage, the TiCu–Al system was irradiated with intense pulsed electron beam on SOLO setup at the energy density of 10, 15, and 20 J/cm^2, pulse duration of 50 and 150 μs, number of pulses of 3–30, and pulse repetition frequency of 0.3 Hz to form Al-based surface alloy saturated with Ti. The TiCuN–AlSi system was irradiated under the same conditions to fuse the hard coating into the substrate. It was supposed that the presence of Ti-based compounds (titanium nitride) in the Al surface layer would increase the strength properties of the material and decrease its wear rate and friction coefficient. The phase composition and defect structure of the modified layers were examined by optical microscopy, scanning microscopy (Philips SEM-515), transmission microscopy (JEOL JEM-2100F), and by X-ray diffraction analysis (XRD 6000 diffractometer, filtered Cu-K$_{\alpha 1}$ radiation, CM-3121 monochromator). The physicomechanical and tribological parameters of the materials were measured using microhardness tester (PMT-3), nanohardness tester (Nanotest-100), high-temperature ball-on-disk tribometer (THT-S-AX0000, ball of diameter 3 mm made of VK8 hard alloy, normal load 5 N, rate of rotation 5 cm/s), and 3D-profilometr (Micro Measure 3D station).

MATHEMATICAL MODEL

The temperature fields which arise during electron beam irradiation are simulated by solving the heat conduction equation for the one-dimension case of heating and cooling of a plate of thickness *d* [10, 11]. The irradiated system comprises massive substrate with a thin wear-resistant coating. The coordinate system is such that the axis ***x*** is directed deep into the specimen. At $x = 0$, heat flux is specified, and the backside of the plate is free from heat exchange. In the coordinate form, the heat conduction equation takes the form [12]:

$$c_p \rho \frac{\partial T}{\partial t} = \lambda \frac{\partial^2 T}{\partial x^2}. \tag{1}$$

Here c_p is the specific heat capacity, ρ is the density, and λ is the heat conductivity of material.

The boundary conditions for pulsed electron beam treatment have the form:

$$-\lambda \frac{\partial T}{\partial x} = q(t), \tag{2}$$

where the heat flux from the surface deep into the specimen is

$$q(t) = \begin{cases} q_0, & 0 < t \le t_0; \\ 0, & t > t_0. \end{cases} \tag{3}$$

Here q_0 is the average heat flux during the time t_0. The initial temperature is $T(0,x) = T_0$ throughout the specimen depth $0 < x < d$.

Because the plate consists of two different materials, we have an additional boundary condition at the interface of two materials: a boundary condition of fourth kind which defines the thermal interaction of the elements differing in thermophysical properties. The equality conditions for the temperatures and heat fluxes on each side of the interface have the form [12]:

$$\begin{cases} -\lambda_1 \left.\dfrac{\partial T_1}{\partial n}\right|_B = -\lambda_2 \left.\dfrac{\partial T_2}{\partial n}\right|_B \\ T_1\big|_B = T_2\big|_B \end{cases} \tag{4}$$

For numerical solution of the problem, we use a difference grid with time and space steps τ and h: $t_j = j\tau$ and $x_i = ih$, where j is the number of a time step and i is the number of a space step. The temperature is determined at the grid nodes. The differential heat conduction equation is approximated with the first order in time and second order in space by an implicit scheme [12]:

$$\left(\frac{\partial T}{\partial t}\right)_{i,j} \approx \frac{T_i^{j+1} - T_i^j}{\tau}, \tag{5}$$

$$\left(\lambda \frac{\partial^2 T}{\partial x^2}\right)_{i,j} = \frac{\lambda}{h^2}(T_{i-1}^{j+1} - 2T_i^{j+1} + T_{i+1}^{j+1}). \tag{6}$$

By using a four-point difference scheme with three points taken at the next time step and one at the previous step, we obtain the following:

$$\begin{cases} T_i^{j+1} = T_i^j + \dfrac{\lambda\tau}{\rho c_p h^2}(T_{i+1}^{j+1} - 2T_i^{j+1} + T_{i-1}^{j+1}),\ i = 2,\dots,n-1;\ \ j = 1,\dots,m-1 \\ T_i^1 = T_0;\ i = 1,\dots n; \\ T_1^{j+1} = T_2^{j+1} + \dfrac{h\cdot q}{\lambda};\ \ j = 1,\dots,m-1; \\ T_n^{j+1} = T_{n-1}^{j+1};\ \ j = 1,\dots,m-1. \end{cases} \tag{7}$$

Thus, the temperature field at the next time step is represented implicitly. For its determination at each internal node we should solve a system of algebraic equations of the form:

$$A_i \cdot T_{i+1}^{j+1} - B_i \cdot T_i^{j+1} + C_i \cdot T_{i-1}^{j+1} = F_i, \tag{8}$$

where $A_i = C_i = \dfrac{\lambda}{h^2},\ B_i = \dfrac{2\lambda}{h^2} + \dfrac{\rho\cdot c_p}{\tau},\ F_i = -\dfrac{\rho\cdot c_p}{\tau}T_i^j,\ i = 2,\dots,n-1$.

At the initial and end point of the computational domain, i.e., at $i = 1$ and at $i = n$, the temperature is determined from the boundary conditions on the left and right walls of the plate, respectively. The system of equations (8) should be solved at each time step for which the sweep method, being a modification of the Gauss method for a three-diagonal matrix, is normally used.

Melting and evaporation is allowed for the following physical consideration [13]. When the melting temperature T_{mel} is reached at a certain point (j, i), the temperature at this point is taken to be fixed and equal to the melting temperature, until the total heat supplied $\left(T_i^j - T_{\text{mel}}\right)c_p$ was equal to melting heat q_{mel} and was assumed to be spent on melting of the specimen. Crystallization is modeled in the same way and so is evaporation and condensation.

The numerical solution of the heat conduction equation was used to calculate the temperature fields in the TiCu–Al system irradiated by an electron beam with an energy density of 10–40 J/cm^2 and pulse duration of 50–200 μs. The surface layer thickness was $d = 10^{-3}$ m, the film thickness was 0.5 μm, the observation time was $t_k = 600$ μs, the time step was 3 μs, and the depth step was 0.05 μm. The calculations were performed for the following thermophysical parameters of titanium [14]: heat conductivity $\lambda = 20\cdot10^{-2}$ W/ (cm·K) and specific heat capacity c_p = $684\cdot10^{-3}$ J/(g·K) both at T = 1000 K; density ρ = 4.5 g/cm^3; melting temperature 1881 K; evaporation temperature 3560 K; melting heat q_{mel} = 358 kJ/kg; evaporation heat q_{ev} = 9720 kJ/kg. The thermophysical parameters of aluminum were the following [12]: heat conductivity $\lambda = 93\cdot10^{-2}$ W/(cm·K) and specific heat capacity c_p = 1177·10^{-3} J/(g·K) both at T = 1000 K; density ρ = 2.6 g/cm^3; melting temperature 933 K; evaporation temperature 2793 K; melting heat q_{mel} = 385 kJ/kg; evaporation heat q_{ev} = 10444 kJ/kg. The thermophysical parameters of titanium nitride were the following [14]: heat conductivity $\lambda = 68\cdot10^{-2}$ W/(cm·K) and specific heat capacity $c_p = 848\cdot10^{-3}$ J/(g·K) both at T = 1000 K; density ρ = 5.13 g/cm^3; melting temperature 3223 K; evaporation temperature 4560 K; melting heat q_{mel} = 1269 kJ/kg; evaporation heat q_{ev} = 12877 kJ/kg. For eutectic silumin, we used the melting temperature of aluminum in AlSi eutectic – 850 K [15].

The calculations revealed irradiation modes in which aluminum is alloyed with titanium both through solid-phase transformation and through liquid-phase mixing of the TiCu film and surface layer of the Al substrate. It is found that in the Ti–Al system exposed to electron beam irradiation for 50 μs, the TiCu film starts melting at E_S = 17 J/cm^2, and the Al substrate starts melting at E_S = 5 J/cm^2 and becomes liquid at E_S = 11 J/cm^2. By the time the TiCu film starts melting (E_S = 17 J/cm^2), the Al substrate has been kept in a two-phase state (solid plus liquid) for 90 μs and in a single-phase state (liquid) for 39 μs; the thickness of its two-phase surface layer is 37 μm and that of the single-phase layer is 19 μm. It is shown that electron beam irradiation of the TiCu–Al system at an energy density of E_S = 10–15 J/cm^2 allows solid-phase doping of aluminum with titanium; liquid-phase mixing of titanium and aluminum is possible at $E_S \geq 17$ J/cm^2. The range of electron beam parameters for fusion of the TiCuN coating into the AlSi substrate was determined. It is shown that the coating is fused in the substrate at $E_s > 10$ J/cm^2 and t_0 = 150 μs.

EXPERIMENTAL RESULTS AND DISCUSSION

TiCu–Al System

Structural analysis of the TiCu–Al system irradiated at E_S = 10 J/cm^2 with N = 10 pulses reveals the presence of Ti fragments separated by Al interlayers on the substrate surface (Fig. 1a). Electron beam irradiation of the TiCu–Al system at E_S = 15 J/cm^2 with N = 3 pulses involves the formation of a submicrocrystalline island structure (Fig. 1b).

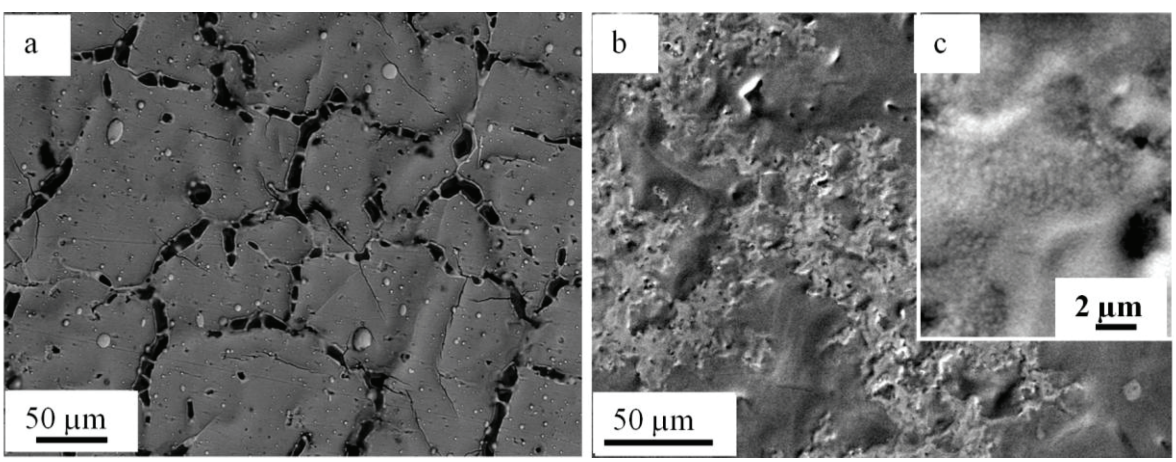

FIGURE 1. Surface structure of the TiCu–Al system irradiated at 10 J/cm^2, N = 10, 50 μs (a) and 15 J/cm^2, N = 3, 50 μs (b, c)

The crystallite size in islands enriched with Al is ≈250 nm (Fig. 1c). X-ray diffraction analysis shows that along with Al and Ti, the surface structure contains Al_3Ti. The volume fraction of Al_3Ti is ≈20 % for irradiation at 10 J/cm^2 with N = 10 and ≈3 % for irradiation at 15 J/cm^2 with N = 3. Hence, the irradiation modes provide thermal conditions for partial dissolution of the TiCu film in the Al substrate at the stage of electron beam heating. Subsequent fast heat removal into the integrally cold substrate involves crystallization of the multicomponent melt and formation of a submicrocrystalline structure.

Irradiation at E_S = 15 J/cm^2 with N = 25 also results in an island structure; however, the surface area occupied by islands enriched in Ti decreases greatly (Fig. 2a) and the main components in the surface layer are polycrystalline islands enriched in Al (Fig. 2b). The Ti-enriched regions are mostly interlayers separating the Al-enriched islands. X-ray diffraction analysis reveals the presence of an Al-based solid solution, Al_3Ti, Ti_3Al, and Ti_3Cu.

The formation of surface alloys provides many-fold increase in the hardness of commercially pure aluminum. For the TiCu–Al system irradiated at 15 J/cm^2, 50 μs, N = 3, 0.3 s^{-1}, the surface hardness increases ~18 times, the wear resistance increases ~1.2 times, and the friction coefficient changes insignificantly.

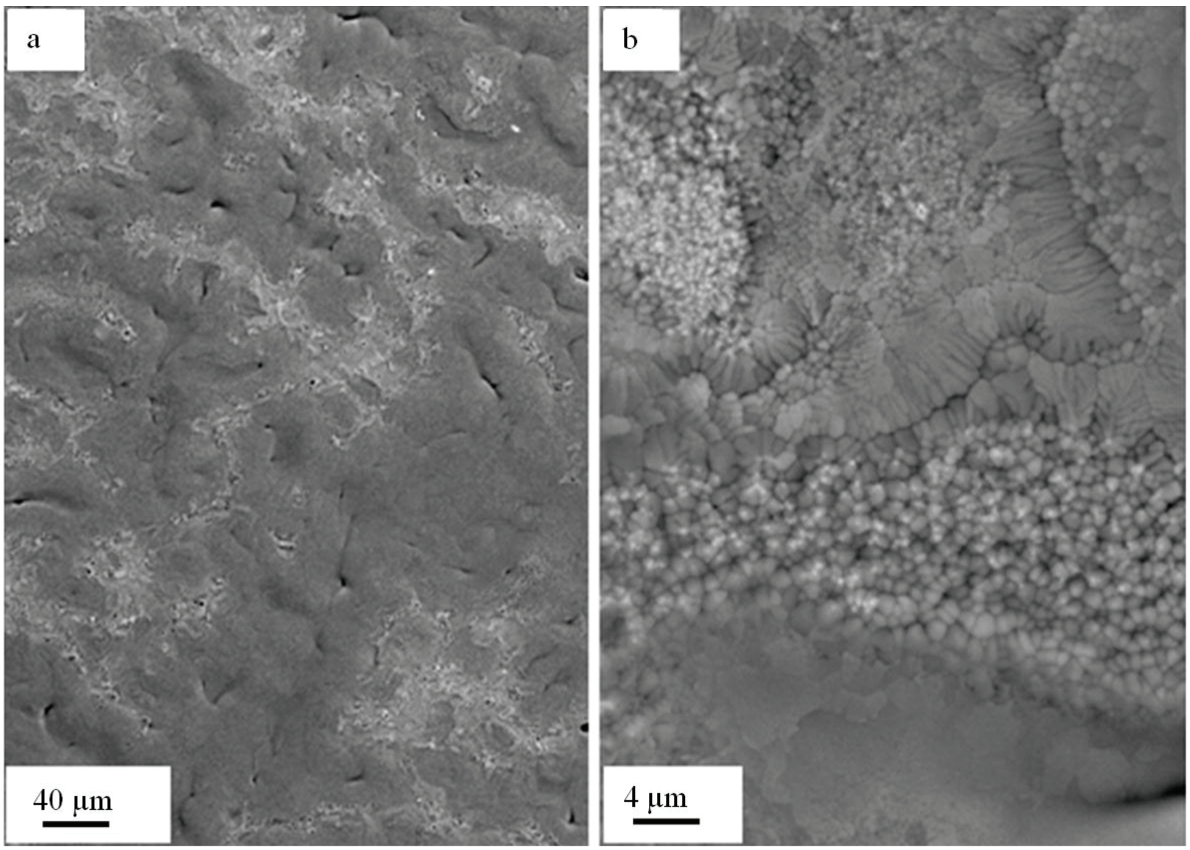

FIGURE 2. Surface structure of the TiCu-Al system irradiated at 16 kV, 15 J/cm^2, 50 μs, N = 25, 0.3 s^{-1}.

TiCuN–AlSi System

Electron beam irradiation of the TiCuN–AlSi system causes microcracking of the hard TiCuN coating such that the space between the coating fragments is filled with Al (Fig. 3b). The latter fact suggests that the coating fragments are fused into the substrate.

Transmission electron microscopy of thin foils provides more detailed data on the surface structure and elemental composition of the irradiated TiCuN–AlSi system. Figure 4a, b shows TEM images of the foil structure in which one can see a crack in the coating (shown by red-white arrows). The distributions of elements in this foil region (Fig. 4c–f) unambiguously suggest that the crack is filled with Al-based alloy containing nanosized Si inclusions.

The TiCuN coating formed on the AlSi surface increases the surface hardness of the system to ≈21 GPa, as evidenced by nanoindentation. After pulsed electron beam treatment, the hardness of the system decreases from 16.6

GPa (10 J/cm^2, N = 3) to 7.9 GPa (15 J/cm^2, N = 3). The hardness of the TiCuN–AlSi system irradiated at 10 J/cm^2, 150 μs, N = 10, 0.3 s^{-1}, which is the best mode in our opinion, decreases to 14.5 GPa but exceeds the hardness of the initial silumin by a factor of ≈60.

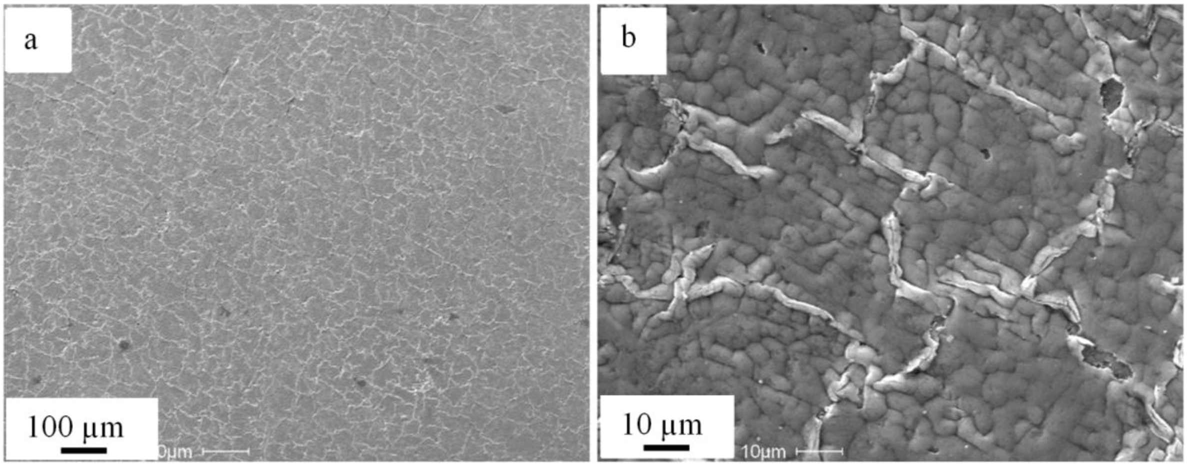

FIGURE 3. Surface structure of the TiCuN–AlSi system irradiated at 10 J/cm^2, 150 μs, N = 10, 0.3 s^{-1}. Scanning electron microscopy

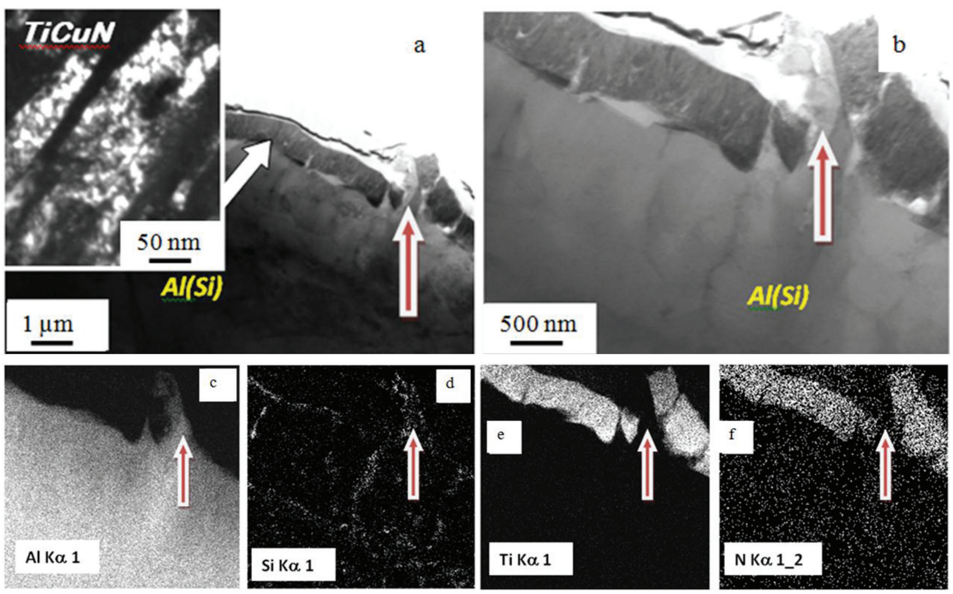

FIGURE 4. TEM images of the surface structure (a, b) and distributions of elements in the TiCuN–AlSi system irradiated at 10 J/cm^2, 150 μs, N = 10, 0.3 s^{-1} (c–f); the coating and the crack in the coating are shown by white and red-white arrows, respectively

Tribological tests of the TiCuN–AlSi system revealed a strong dependence of its wear resistance and friction coefficient on the irradiation mode. The optimum mode for the TiCuN–AlSi system is electron beam irradiation at an energy density of 10 J/cm^2 with N = 10 pulses. In this case, the wear resistance of the material increases ≈2.2 times compared to silumin with no coating, and the friction coefficient decreases ≈2.0 times. It should be noted that the wear resistance of the TiCuN–AlSi system irradiated in the optimum mode is ~2.6 times higher than that of the system before electron beam irradiation.

CONCLUSION

The one-dimensional model used in the study allowed us to determine the temperature field and the irradiation modes which provide alloying of aluminum with titanium through solid-phase transformation and through liquid-phase mixing of the TiCu film and Al surface layer and those which provide fusion of the TiCuN coating in the AlSi surface layer. It is shown that melting and subsequent high-rate crystallization of the TiCu–Al system makes possible a multiphase surface structure with a crystallite size ranging within micrometer, hardness of more than 3 times that in the material bulk, and wear resistance ≈1.8 times higher compared to the initial material. It is found that irradiation of the TiCuN–AlSi system by a submillisecond intense pulsed electron beam provides fusion of the coating in the substrate. Electron beam irradiation at 10 J/cm^2, 50 μs, N = 10, 0.3 s^{-1} increases the wear resistance of the TiCuN–AlSi system ~2.2 times and decreases its friction coefficient ~2.0 times at a surface hardness of ~14 GPa.

ACKNOWLEDGMENTS

The research is conducted within the grant of the Russian Science Foundation (project No. 14-29-00091).

REFERENCES

1. F. I. Kvasov and I. N. Fridlyander, *Commercial Aluminum Alloys* (Metallurgia, Moscow, 1984), 528 p. (in Russian).
2. V. M. Beletsky and G. A. Krivov *Aluminum alloys* (Komintekh, Moscow, 2005), 365 p. (in Russian).
3. B. Guo, J. Zhou, S. Zhang, H. Zhou, Y. Pu and J. Chen, Appl. Surf. Sci. **253**, 9301–9310 (2007).
4. S. Romankov, A. Mamaeva, S. D. Kaloshkin and S. V. Komarov, Mater. Lett. **61** (39), 5288–5291 (2007).
5. I. A. Kurzina, E. V. Kozlov, Yu. P. Sharkeev, S. V. Fortuna, N. A. Koneva, I. A. Bozhko and M. P. Kalashnikov, *Nanocrystalline intermetallic and nitride structures formed by ion beam treatment* (Izd. Nauch. Tekh. Lit., Tomsk, 2008), 324 p. (in Russian).
6. L. Illecova, J.C. Gachon, A. Rogachev, H. Grigoryan, J. C. Schuster, A. Nosyrev and P. Tsygankov, Thermochimica Acta **469,** 77–85 (2008).
7. E. B. Berlin, N. N. Koval and Seidman L.A., *Thermochemical plasma treatment of steel surfaces* (Tekhnosfera, Moscow, 2012), 464 p. (in Russian).
8. V. V. Uglov, G. E. Remnev, A. K. Kuleshov and V. M. Astashinski, Surf. Coat. Technol **204,** 1952–1956 (2010).
9. N. N. Koval and Yu. F. Ivanov, Izv. Vyssh. Uchebn. Zaved. Fiz. **5**, 60–70 (2008). (in Russian).
10. Yu. F. Ivanov, N. N. Koval, V. I. Vlasov, A. D. Teresov, E. A. Petrikova, V. V. Shugurov, O. V. Ivanova, I. A. Ikonnikova and A.A. Klopotov, High Temperature Material Processes 17(4), 241–256 (2013).
11. Yu. F. Ivanov, E. A. Petrikova, O. V. Ivanova, I. A. Ikonnikova, A. D. Teresov, V. V. Shugurov and O. V. Krysina, Russian Physics Journal, **58**, No. 3, July, 366-372 (2015) (Russian Original No. 3, March, 2015).
12. G. B. Kuznetsov and M. A. Sheremet, *Difference methods for solving heat conduction problems* (TPU Publishing, Tomsk, 2007), 187 p. (in Russian).
13. V. Rotshtein, Yu. Ivanov and A. Markov, "Surface treatment of materials with low-energy, high-current electron beams," Ch. 6 in *Materials surface processing by directed energy techniques*, edited by Y. Pauleau (Elsevier, Paris, 2006), pp. 205-240.
14. A. P. Babichev, N. A. Babushkina and A. M. Bratkovsky, *Physical quantities* (Energoatomizdat, Moscow, 1991), 1232 p. (in Russian).
15. A.E. Vol, *Structure and properties of binary metal systems. V.1.,*(Gos. Izd. Fiz. Mat. Lit., Moscow, 1959), 755 p. (in Russian).